

Chemical Communications

Submitted: 2016 May

Supplementary Information

Polyaniline Films Photoelectrochemically Reduce CO₂ to Alcohols

Dorottya Hursán^{1,2}, Attila Kormányos^{1,2,3}, Krishnan Rajeshwar^{3,4*}, and Csaba Janáky^{1,2*}

Affiliations:

¹Department of Physical Chemistry and Materials Science, University of Szeged, Szeged,
Hungary.

²MTA-SZTE „Lendület” Photoelectrochemistry Research Group, Rerrich Square 1, 6720,
Szeged, Hungary.

³Department of Chemistry and Biochemistry, University of Texas at Arlington, Arlington, Texas,
USA.

⁴Center for Renewable Energy Science & Technology, University of Texas at Arlington,
Arlington, Texas, USA.

*Correspondence to: rajeshwar@uta.edu (K.R.) and janaky@chem.u-szeged.hu (C.J.)

Table of Contents

- 1. Band edge positions of different SCs employed in PEC CO₂ reduction*
- 2. PEC behavior of PANI under simulated solar irradiation*
- 3. Long term photoelectrolysis*
- 4. PEC behavior of other conducting polymers*
- 5. Electrochemical behavior of the studied CPs*
- 6. PANI/CNT composites for enhanced performance*
- 7. Electrosynthesis of the studied polymers*
- 8. Materials and Methods*

1. Band edge positions of different SCs employed in PEC CO₂ reduction

The CO₂-reducing ability of the photogenerated electrons is dictated by the position of their surface quasi-Fermi level and the SC conduction band edge. Comparison of the band structure of the reported inorganic SCs and conducting polymers studied in this paper (Fig. S1).

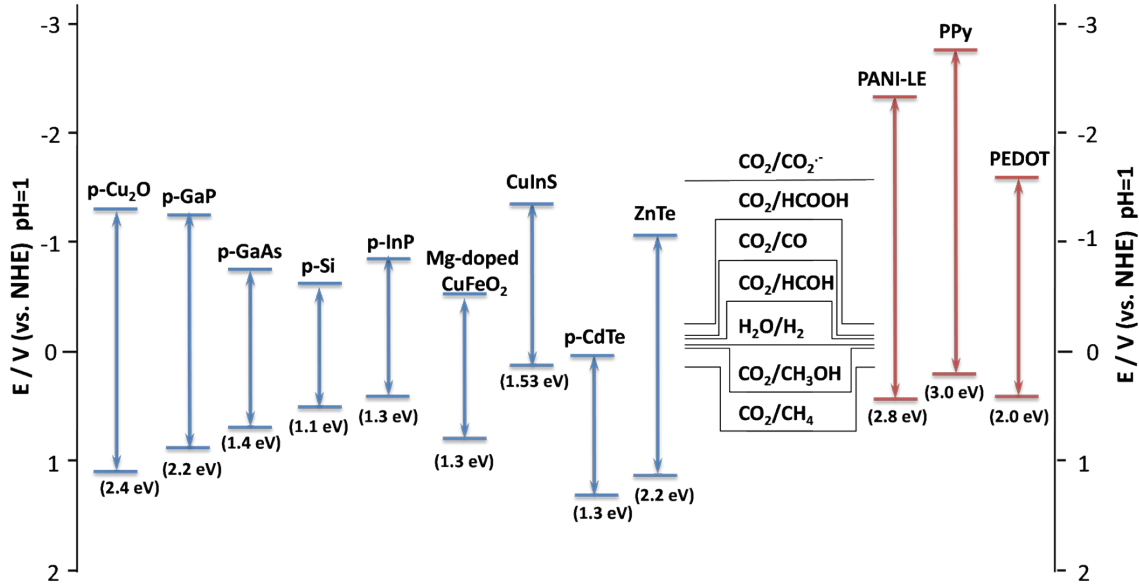


Fig. S1. Comparison of the band edge positions of the most frequently employed inorganic semiconductors and the conducting polymers investigated in this study.

2. PEC behavior of PANI under simulated solar irradiation

Photovoltammograms of the PANI film were also recorded by irradiating the photocathode with simulated sunlight yielding very similar profiles to those reported in the main text both in terms of shape and absolute photocurrent values (Fig. S2).

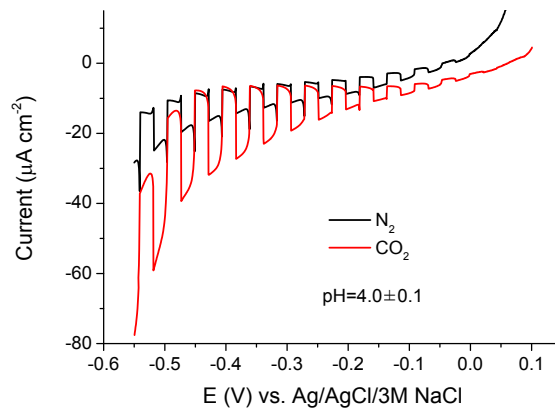


Fig. S2. Representative photocurrent-potential profiles for an electrodeposited PANI layer under simulated sunlight illumination (100 mW cm⁻²) in (A) N₂- and CO₂-saturated 0.1 M Na₂SO₄ aqueous solution (pH=4.0±0.1).

3. Long term photoelectrolysis

During the long term photoelectrolysis, an initial decrease in the photocurrents was always observed (see also in Fig. 2C in the main text). At the same time, the intrinsic *electroactivity* of the PANI films did not change significantly (as probed by cyclic voltammetry before and after photoelectrolysis, see Fig. S3). This fact confirms that no a molecular or supramolecular degradation is the process behind the decrease of the PEC performance. Scanning electron microscopic images (SEM) furnished insights on this peculiar phenomenon, namely that the decrease in the PEC activity is predominantly rooted in the melting of the polymer (Fig. S4).

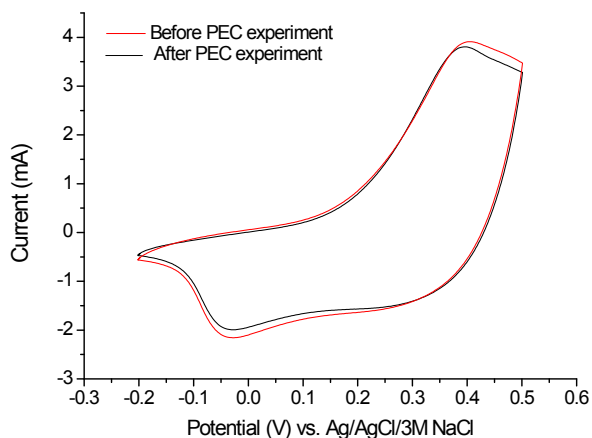


Fig. S3. CV traces registered in 0.1 M Na_2SO_4 in water at 100 mVs^{-1} scan rate, for a PANI film, before and after performing photoelectrolysis (as in Fig. 2C in the m-s text).

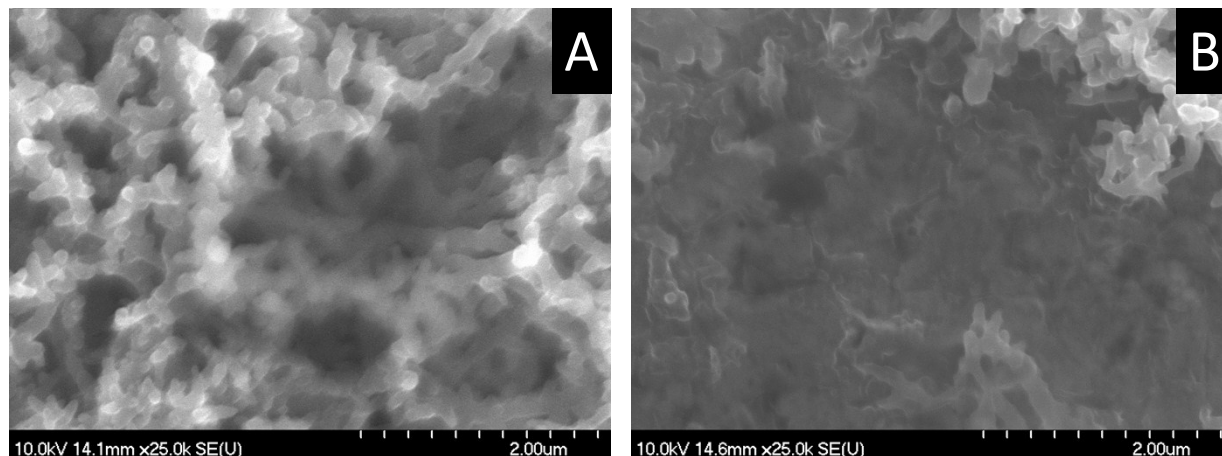


Fig. S4. SEM images of electropolymerized PANI films (with a charge density of 150 mC cm^{-2}), before (A) and after (B) a 2 h CO₂ photoelectrolysis at $E=-0.4 \text{ V}$. Continuous UV-Vis illumination (Xe-Hg Arc lamp, 300 W output) was employed.

4. PEC behavior of other conducting polymers

Linear sweep photovoltammetry was also performed with polypyrrole (PPy), poly(3,4-ethylenedioxythiophene) (PEDOT), and poly(N-methylaniline) electrodes. As seen in Fig. S5 these showed only negligible photoeffects from CO₂ reduction.

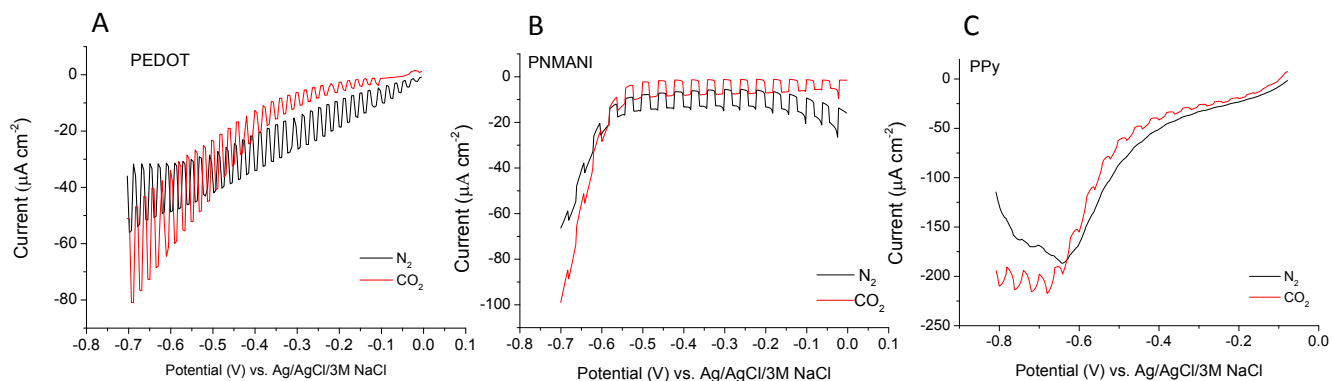


Fig. S5. Representative photocurrent-potential profiles of an electrodeposited PEDOT (A), PNMANI (B), and PPy (C) layers under chopped UV-vis illumination (Xe-Hg Arc lamp, 100 W output) in (A) N₂- and CO₂-saturated 0.1 M Na₂SO₄ aqueous solution.

5. Electrochemical behavior of the studied CPs

The intrinsic electroactivity of the studied polymers was also evaluated. The potential regime was identified where conducting polymers behave as a SC (rather than as a semi-metal). This behavior is associated with the fully reduced state of the polymers, indicated with arrows on Fig. S6. At more positive potentials, the polymer electroactivity would dominate of the CO₂ conversion, as exemplified here by the PPy case.

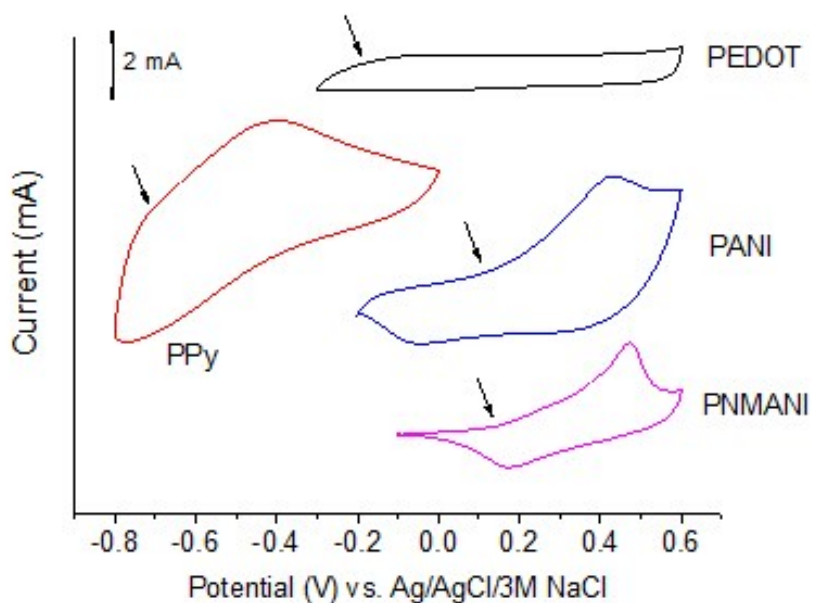


Fig. S6. CV traces registered in 0.1 M Na₂SO₄ in water at 100 mVs⁻¹ scan rate, for a PEDOT, PPy, PANI and PNMANI. The arrows indicate the onset potential value used for electrochemical oxidation.

6. PANI/CNT composites for enhanced performance

To increase the specific surface area of the photocathode, PANI was deposited on a carbon nanotube network (see Fig. S7 for SEM images). With identical PANI amount, strikingly higher photocurrents (up to 0.5 mA cm^{-2}) were obtained, because of the better charge separation/transport (Fig. S8).

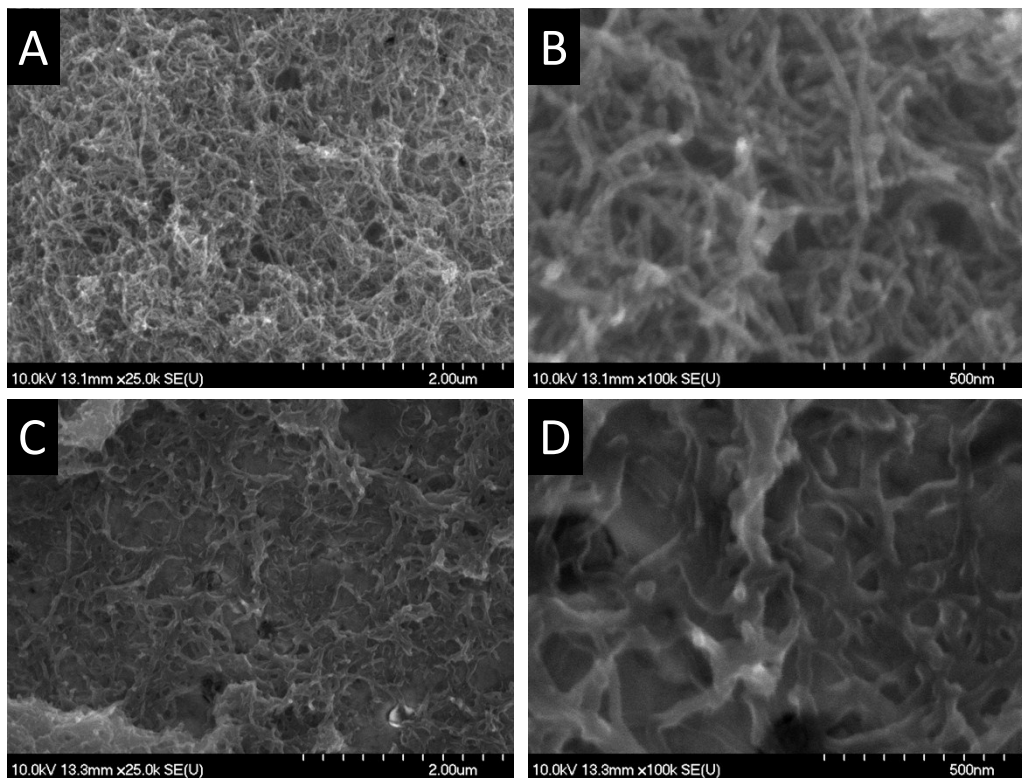


Fig. S7. SEM images of the spray coated CNTs, before (A, B) and after (C, D) PANI electrodeposition. PANI was electropolymerized via potentiodynamic cycling, with a charge density of 150 mC cm^{-2} .

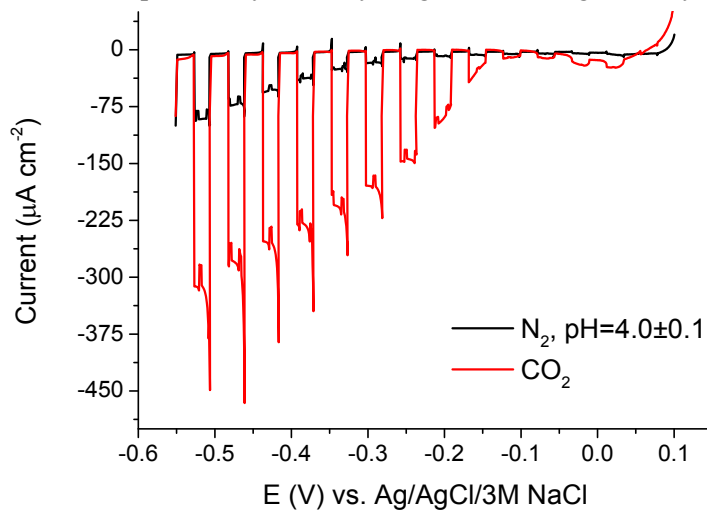


Fig. S8. Representative photocurrent-potential profiles for an electrodeposited CNT/PANI layer under chopped UV-vis illumination (Xe-Hg Arc lamp, 300 W output) in (A) N_2 - and CO_2 -saturated 0.1 M Na_2SO_4 aqueous solution (pH = 4.0 ± 0.1).

7. Electrosynthesis of the studied polymers

All polymers were electropolymerized on a gold supporting electrode from the respective monomers and the employed method was tailored to each monomer (Fig. S9).

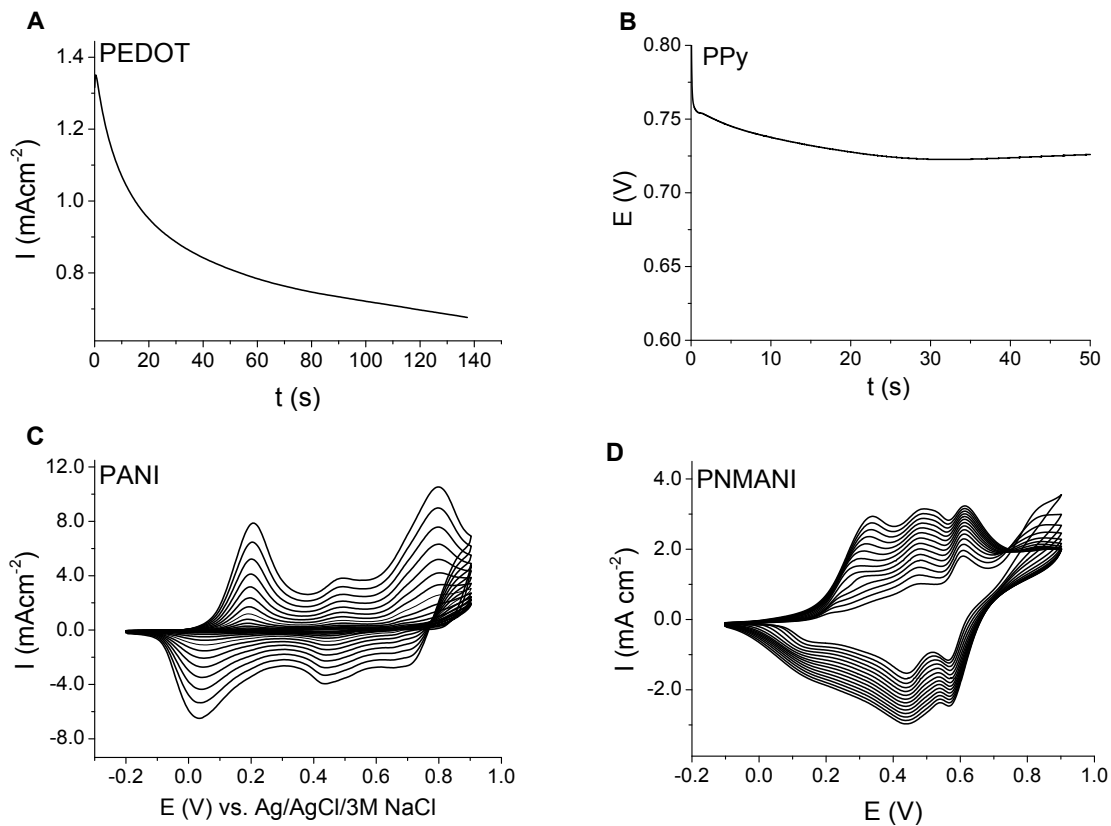


Fig. S9. Representative polymerization curves for the studied polymers. (A) 0.01 M EDOT; 0.05 M Na-dodecyl-sulfate; $E = 1.1$ V; (B) 0.1 M pyrrole, 0.05 M Na-dodecyl-sulfate; $i = 3$ mA cm⁻² (C): 0.2 M aniline, 0.5 M H₂SO₄; 100 mV s⁻¹ (D): 0.1 M N-methylaniline; 1.0 M HClO₄; 100 mV s⁻¹. All polymers were deposited with a charge density of 150 mC cm⁻².

8. *Materials and Methods*

Polymer synthesis. All chemical reagents used in the study were of analytical grade and were used without further purification, except the monomers, which were freshly distilled before use. All polymers were electropolymerized on a gold supporting electrode from the respective monomers and the employed method was tailored to each monomer. Electropolymerization was carried out in a conventional single-compartment, three-electrode electrochemical cell, using an Autolab PGSTAT 302 system with Au foil, Pt foil, and Ag/AgCl/3M NaCl as working, counter and reference electrodes, respectively. Representative polymerization curves are shown in Fig S9.

PANI was also electrodeposited on MWCNT films. First the nanotubes were spray-coated to the supporting gold electrode, and PANI was subsequently electrodeposited using the same polymerization charge as for the flat films.

CO₂-adsorption studies. Carbon dioxide adsorption on the polymer films was monitored by the quartz crystal microgravimetry (QCM) technique using a Stanford Research Systems QCM 200 instrument. The polymer films were deposited using a charge density of 100 mC cm⁻² on gold-coated quartz crystal (5 MHz resonance frequency). The polymer films were first incubated in N₂ for 30 min; then the atmosphere was periodically changed from N₂ to CO₂ and vice versa every 5 min in a sealed cell. The mass changes were calculated from the measured frequency changes using the calibration constant of the crystal.

Vibrational spectroscopic changes upon CO₂ adsorption were monitored by FT-IR spectroscopy using an Agilent 670 Fourier transform infrared spectrometer equipped with a Harrick's Praying Mantis™ Diffuse Reflection Accessory. All infrared spectra were recorded between 6000 and 600 cm⁻¹, at 2 cm⁻¹ optical resolution, by averaging 16 interferograms. The background spectra were recorded at room temperature after a 60 min pretreatment in He, at 200 °C. Subsequently, the chamber was purged with CO₂ and a series of IR spectra were recorded with increasing contact time. Finally, He was purged to the chamber again, and IR spectra were recorded.

Photoelectrochemical measurements. All photoelectrochemical measurements were performed on an Autolab PGSTAT302 instrument in a custom designed two-compartment and three-electrode photoelectrochemical cell. The conducting polymer coated gold electrode was always used as working electrode, while a large Pt foil and a Ag/AgCl/3M NaCl, along with the working electrode, completed the cell setup. All PEC measurements were reproduced using a glassy carbon counterelectrode and no difference was revealed. This shows that any products electrogenerated at the Pt electrode (e.g., protons) do not interfere with the photoreduction process. The light source was a 100-300 W Hg-Xe arc lamp (Hamamatsu L8251). The radiation source was placed 8 cm away from the working electrode surface which was irradiated through a quartz window. The electrolyte used was 0.1 M Na₂SO₄. Solutions were saturated with N₂ or with CO₂ as needed by 30 min continual bubbling through the sealed cell. For comparative studies, the pH of the N₂-saturated solution was adjusted to pH = 4.0±0.1 using phosphate buffer. LSV curves were also recorded in pH=7 solutions (N₂ / 0.1M Na₂SO₄ and CO₂ / 0.1M NaHCO₃) for additional comparison. For some comparative measurements a Newport LCS- 100 solar simulator was also used, applying 1 Sun irradiance with an AM1.5G filter.

Photovoltammograms were obtained using a slow potential sweep (2 mV s⁻¹) in conjunction with interrupted irradiation (0.1 Hz) on the semiconductor film electrodes. For the chronoamperometric measurements, the working electrode was set at pre-selected potential

values (e.g., -0.4 V), and the photocurrent transients under illumination were monitored for 30 s. All procedures described below were performed at the laboratory ambient temperature (25 ± 2 °C).

The IPCE was calculated by normalizing the photocurrent values for incident light energy and intensity by use of the equation, i.e., $IPCE(\%) = 100 \times 1240 \times I_{\text{photo}} / (I_{\text{inc}} \times \lambda)$ where I_{pc} is photocurrent (mAcm^{-2}), I_{inc} is the incident light intensity (mWcm^{-2}) and λ is the wavelength (nm).

CO₂ photoelectrolysis. Bulk photoelectrolysis at $E = -0.4$ V vs. Ag/AgCl/3M NaCl was also performed in a two-compartment sealed electrochemical cell under continuous light irradiation using the above mentioned equipment. Liquid aliquots were taken at the end of photoelectrolysis to be analyzed in a gas chromatograph equipped with a mass spectrometer as detector (GC-MS). The aliquots were injected into the Shimadzu GC-MS 2010SE chromatograph coupled with a MS QP2010 detector. The chromatographic column was Stabilwax-DA (30 m length and 0.32 mm inner diameter) set at 40 °C, the gradually reached injection temperature was 220 °C. The MS detector was set at 200 °C, and helium was used as the carrier gas. Qualitative detection was afforded by selective ion monitoring (SIM)-MS, while the total ion chromatogram was used for the quantification of methanol and ethanol.